

Bismuth and antimony on GaAs(110): Dielectric and electronic properties

Maria Grazia Betti and M. Pedio

Istituto di Struttura della Materia, CNR, via Enrico Fermi 38, I-00044 Frascati, Italy

U. del Pennino and Carlo Mariani

Dipartimento di Fisica, Università di Modena, via G. Campi 213/A, I-41100 Modena, Italy

(Received 13 August 1991)

An investigation of the metal-induced electronic states, the dielectric properties, and the growth morphology of Bi/GaAs(110) and Sb/GaAs(110)—as model systems, for epitaxial and unreactive interfaces—is presented. The electronic transitions involving surface and Bi (Sb)-induced states, investigated by means of high-resolution electron-energy-loss spectroscopy, are discussed and compared with previous results. In the Bi/GaAs(110) interface, a clear absorption structure appears within the bulk gap, revealing its semiconducting character with a surface gap of 0.65 eV at one monolayer. When an ordered monolayer of Sb is formed, only a slight shift of the absorption edge is observed and the interface shows semiconducting properties. At higher coverages, the different growth morphology and dielectric properties of the Bi/GaAs(110) and the Sb/GaAs(110) interfaces are discussed. Above the first epitaxial and semiconducting monolayer, Bi builds up in a regular structure with a metallic dielectric character before approaching a bulklike crystalline and semimetallic behavior, while Sb grows as an amorphous and semiconducting layer before becoming polycrystalline and semimetallic.

INTRODUCTION

Although the study of the surface electronic structure of semiconductor-metal interfaces has been the subject of innumerable works in the past few years, a clear understanding of the interrelationship between the electronic properties and the growth morphology is still lacking. In fact, semiconductor-metal interfaces often react disruptively and interdiffusion processes characterize the growth morphology. A good lattice registry between the metal overlayer and the semiconductor substrate, as well as a sharp and unreactive interface without intermixing are the essential requirements to drive an epitaxial and ordered growth with a clear atomic topography at the interface.

The microscopical ordering and the geometrical arrangement at the interface are strictly related to the overlayer-induced electronic states and to the dielectric properties of the metal-semiconductor interfaces.

Group-V semimetal chemisorption on the (110) surface of III-V semiconductor compounds is a valuable model that can provide an opportunity to correlate structural and electronic properties at the interface. In fact, an ordered and stable (1×1) structure, with a one-to-one correspondence between the substrate and overlayer atoms, can be grown when one semimetal monolayer is deposited on the cleavage surface of III-V semiconductor compounds. In particular antimony and bismuth atoms are arranged along the atomic chains in the $[1\bar{1}0]$ direction with the same geometry as the atoms of the topmost III-V layer.¹⁻⁸

The semimetal ordered overlayer has been a prototype for experimental works which can take advantage of extensive theoretical support^{7,8} as it concerns atomic position determination, nature of the bonding at the inter-

face, as well as energy position of the induced electronic states.

For the Sb/GaAs(110) system, low-energy electron diffraction (LEED) experiments¹ established the geometry of the Sb commensurate adlayer with a one-to-one correspondence between the topmost GaAs layer and the Sb atoms. Scanning tunneling microscopy (STM) studies⁴ confirmed the structural results, shedding light on the atomic topography at the interface.

Scanning tunneling microscopy^{5,6} revealed that one monolayer of bismuth is not a fairly well commensurate adlayer system on GaAs(110). At one monolayer, periodic series of Bi atoms are missing in the direction perpendicular to the atomic chains and the average separation of these rows of dislocations is about 25 Å. The origin of such dislocations can be ascribed to a mismatch in lateral size between the Bi overlayer and the GaAs(110) substrate. Dislocations are absent in the STM images of Sb on GaAs(110) and this is consistent with the larger atomic radius of Bi compared to Sb.

The regular dislocation arrays generate dangling and broken bonds⁵ which can influence the electronic properties. In fact, acceptorlike states are present within the gap, close to the missing Bi atoms, even when one monolayer of Bi on GaAs(110) is completed, while, for the Sb/GaAs system, additional states were attributed to the land edges at the submonolayer coverages but disappeared at the completion of one monolayer.⁴

Since Sb and Bi are isoelectronic and structural investigations showed analogies in the ordered growth near a monolayer (ML) coverage, a similar evolution of the electronic properties might be expected.

Band-structure calculations,^{7,8} angle-resolved photoemission,⁹ and inverse photoemission¹⁰ investigations for (1 ML Sb)/GaAs(110) interface indicated the existence of

Sb-induced filled states (S5 and S6) below the valence-band maximum (VBM), and empty levels (S7 and S8) close to the conduction-band minimum (CBM). Calculations based on the pseudopotential approach⁷ localized the S5 and S6 states on the overlayer plane without any contribution from the internal planes, probably due to the lone pairs of the Sb atoms with the maxima of the charge pointing out of the surface. In the upper region of the valence band, two further states, labeled S3 and S4, are related to Sb-As and Sb-Ga coupling, respectively. Even though tight-binding calculations⁸ used the same atomic geometry, they found that the S5 and S6 Sb-induced filled states have a π bonding character and give rise to the bonding of the Sb chains to the substrate. Both calculations found the empty S7 and S8 levels as the antibonding counterpart of the filled states involved in the bonding between Sb and the substrate atoms.

Currently, band-structure calculations for the Bi/GaAs(110) interface are still lacking. Although the semimetal-induced states have different energy positions in (1 ML Sb)/GaAs(110) and in (1 ML Bi)/GaAs(110), the scheme of the energy levels shows strong similarities.^{5,6,9,11} In fact, for 1 ML of Bi on GaAs(110), angular resolved photoemission spectra¹¹ displayed two states within the bulk gap and the scanning tunneling spectroscopy results^{5,6} showed filled (S5 and S6) and empty (S7 and S8) Bi-induced states separated by a band gap of about 0.7 eV. Inverse photoemission data^{12,13} found two unoccupied Bi-induced states and assigned these states to the outer Bi-Bi bonding and to the inner Bi-GaAs interfacial layers, respectively. Hu *et al.*¹³ observed a strong Bi-derived empty state at 1.25 eV above the Fermi energy (E_F), and for coverages higher than one monolayer at 0.35 eV above E_F .

The structural similarity of the epitaxial monolayer formation for the Sb/GaAs(110) and Bi/GaAs(110) interfaces is reflected in the electronic properties. The room-temperature (RT) growth and the corresponding dielectric nature of the semimetal thicker layers of Sb and Bi on GaAs(110) differ considerably.

For the Sb/GaAs(110) system, after the completion of one monolayer, a three-dimensional amorphous island growth takes place without interdiffusion in the substrate.¹⁴⁻¹⁶ As previously discussed by Annovi *et al.*,¹⁴ the amorphous clustering has a semiconducting behavior up to coverages of about 15 ML, when a transition towards a polycrystalline phase takes place and metallic islands start to form. Eventually the metallic islands coalesce into a fully polycrystalline semimetallic bulklike layer. The only direct link between amorphous structure and the evolution of the electronic states in the high-coverage range (2–10 ML) has been provided by scanning tunneling spectroscopy.¹⁷

The growth morphology of the thick Bi layer shows a different behavior with respect to the thick Sb layer. After the completion of the semiconducting monolayer, a Stranski-Krastanov growth starts and good LEED images are preserved, ensuring a crystalline growth. Nevertheless controversy exists as regards the presence of superstructures in the LEED patterns. Ludeke *et al.*⁵ and Joyce *et al.*¹⁸ did not observe any significant change in

the (1×1) LEED pattern at different Bi coverages, while a new superstructure, consisting in extra spots oriented in the $[1\bar{1}1]$ and $[\bar{1}11]$ directions, between 2 and 10 ML, was observed by other authors.^{12,13,19} The presence of this intermediate crystalline phase up to 10 ML was also stressed by Raman spectroscopy^{19,20} and its semimetallic behavior was revealed by inverse photoemission results.¹³ Beyond 20–30 ML the crystalline thick Bi layer grows with a hexagonal bulklike symmetry.^{13,19}

The aim of this work is a study of the electronic and dielectric properties in the energy region of the bulk gap for Bi and Sb deposited on GaAs(110), in order to further enlighten the interrelationship between the electronic structure and the growth morphology of these systems. The high-resolution electron-energy-loss spectroscopy (HREELS) was used in a wide energy-loss range (0–4000 meV), focusing attention on different spectral structures relating to vibrational and electronic excitations.

In fact, high-resolution electron-energy-loss spectroscopy is a surface-sensitive technique well suited for studying both vibrational and electronic properties of clean semiconductor surfaces and ultrathin films.^{14,22-28} Its high energy resolution in a wide energy range allows investigations of the evolution of surface and overlayer-induced states in the energy region of the semiconductor bulk gap. In the past, several works were dedicated to studying the electronic and vibrational properties of the clean semiconductor surfaces by means of HREELS.²¹⁻²³ The ordered semimetallic overlayers are prototypic systems for extending the investigation to metal-semiconductor interfaces, highlighting the origin of the surface and overlayer-induced electronic states in the semiconductor bulk gap.²⁶⁻²⁸

In the following section, after a description of the experimental apparatus, a complete study of the Bi- and Sb-induced electronic states for the (1×1) Bi and Sb monolayer is presented. We will focus attention to the overlayer-induced electronic states involved at different stages of the monolayer formation both as deposited at RT and after adequate annealing procedures of the thick semimetal film.

In the second part, the differences in the growth morphology of thicker Bi and Sb overlayers will be discussed and compared with their respective dielectric and electronic properties. The evolution of the substrate vibrational properties and the variation in the reflectivity of the scattered electrons will give important information about the dielectric nature of the overlayers.

EXPERIMENT

The HREEL experiments were performed in the surface physics laboratory Spettroscopia Elettronica Superfici ed Adsorbati (Sesamo) at the Dipartimento di Fisica, Università di Modena. Measurements were performed in an ultrahigh-vacuum (UHV) system constituted by two chambers, one containing a high-resolution monochromator-analyzer spectrometer (Leybold Heraeus ELS 22), equipped with LEED and x-ray photoemission spectroscopy (XPS) instrumentation, the other containing all the ancillary equipment for sample preparation.

The base pressure in the main chamber was kept below 7×10^{-11} mbar (7×10^{-9} Pa). The GaAs single crystals were *n*-type doped ($n \sim 3 \times 10^{17}$ cm⁻³) bars and the (110) clean surfaces were obtained by cleaving *in situ*, with a single wedge technique. After cleavage, the surface crystalline order was checked by observing the LEED pattern. The surface cleanliness was monitored by measuring the absence of any contaminant, in particular the C-H stretching frequency.

Bismuth was evaporated from Bi flakes contained in a resistively heated quartz crucible and the evaporation rate was kept at about 0.5 ML/min. The Sb shots were sublimated following the same procedure. The pressure in the preparation chamber, during the Sb and Bi depositions, rose to 2×10^{-10} mbar. Thickness was measured by means of a quartz crystal-thickness monitor. One monolayer was defined as 8.85×10^{14} atoms/cm², equating the density of surface atoms of GaAs(110). Before the HREEL experiment, an XPS analysis was performed in order to check the Bi and Sb deposition.

One monolayer of semimetal was obtained with appropriate annealing procedures. We deposited 4 ML of Sb (Bi) and heated the GaAs crystal at about 300°C (270°C) for about 15 min, with a resistively heated tungsten wire positioned close to the bar and out of sight of the surface. The temperature was monitored with a Chromel-Alumel thermocouple welded close to the surface.

All HREELS measurements were performed in the specular direction geometry at grazing angle of incidence of 65°. The plane of scattering was oriented along the [110] direction of the surface Brillouin zone.

RESULTS AND DISCUSSION

The HREEL data in the energy-loss region of the semiconductor bulk gap for the clean GaAs(110) surface and after Bi and Sb deposition are reported in Figs. 1(a) and 1(b), respectively.

For the Bi/GaAs(110) interface a (1×1) LEED pattern was clearly detected in the coverage range 0.2–1 ML with a slight background with respect to the clean surface.

In Table I we report the energy positions of the loss structures—as deduced from a numerical second derivative of the data—for the Bi/GaAs interface at different Bi coverages.

The energy position of the absorption edge for the clean surface is coincident with the bulk gap at 1.41 eV [Fig. 1(a)],²⁹ as previously reported by del Pennino *et al.*,²³ and indicates the absence of surface states in the bulk gap. After the first Bi deposition (0.2 ML) the gap narrows at less than 0.6 eV and a few structures appear within the semiconductor bulk gap and persist up to the completion of one monolayer. The first clear peak has a maximum at 0.85 eV. Since the S5 and S6 filled Bi-induced states have been singled out at 0.11 and 0.54 eV above the VBM, in the Γ point of the surface Brillouin zone (SBZ) by angle-resolved photoemission,¹¹ we can assign this feature to an electronic transition between the filled S6 and the empty S7 Bi-induced levels. This elec-

tronic transition, involving the S7 empty final state, has a clear intensity increasing above 0.5 ML. In inverse photoemission studies,¹² the empty S7 state was detected only after the completion of the first monolayer and therefore it has been related to a Bi-Bi bond. The bump at 1.2 eV

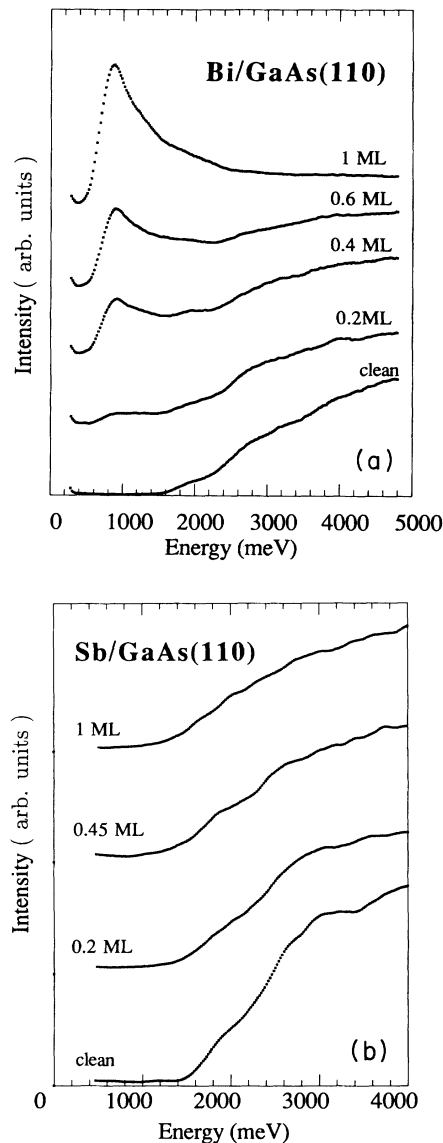


FIG. 1. (a) High-resolution electron-energy-loss spectra of the Bi/GaAs(110) system as a function of Bi coverage (0.2–1 ML) in the energy region of the fundamental bulk gap. Primary beam energy $E_p = 15.9$ eV; angle of incidence $\theta_i = 65^\circ$. Spectra are normalized to the respective elastic peak heights and displaced along the vertical axis for convenience. The counting rate for the anelastic cross section, in this energy range, is about 100 counts/sec. (b) High-resolution electron-energy-loss spectra of the Sb/GaAs(110) system, as a function of Sb coverage (0.2–1 ML) in the energy region of the fundamental bulk gap. Primary beam energy $E_p = 15.9$ eV; angle of incidence $\theta_i = 65^\circ$. Spectra are normalized to the respective elastic peak heights and displaced along the vertical axis for convenience. The counting rate, for the anelastic cross section, in this energy range is about 15 counts/sec.

TABLE I. Energy positions of the loss structures for Bi/GaAs(110) at different coverages as deduced by a numerical second derivative of the data reported in Figs. 1(a) and 2(b).

Bi/GaAs(110)			
Clean			1.9
0.2 ML	0.85	1.2	1.9
1 ML	0.85	1.2	1.9
4 ML annealed	0.80	1.2	1.8

can be ascribed to a transition from the filled S5 to the empty S7 levels and a third broad feature, lying at 1.9 eV, involves S6 and S8 Bi-induced states.

All the electronic transitions present after the first Bi deposition persist when the monolayer is formed and these results are in favor of an electronic picture where the Bi antibonding states are due to the Bi-Ga and Bi-As bondings, as described in the analogous Sb/GaAs(110) interface by band-structure calculations.^{7,8}

In the Sb/GaAs(110) interface, after the first Sb deposition, a slight tail appears towards lower energy losses, as shown in Fig. 1(b). At 0.45 ML a slight shift of the absorption edge is present and the tail increases in intensity, revealing the presence of a joint density of states between levels induced in the gap, probably due to defects and/or disorder. At one monolayer the absorption feature is almost structureless and only after the annealing procedure, described below, are clear structures in evidence.

The ordered monolayer was obtained after depositing 4 ML and heating the GaAs crystal at about 300°C for about 15 min. At 4 ML the LEED presents a (1×1) pattern superimposed on a structureless background. After the annealing treatment, the (1×1) LEED pattern appears with sharp and distinct diffraction spots. The resulting more ordered (1×1) structure causes a higher elastic cross section—as measured by the elastic peak intensity—with respect to the 1 ML of Sb as deposited.

The HREEL spectra obtained after the proper annealing procedure of the Sb/GaAs(110) interface are shown in Fig. 2(a). The energy positions of the HREEL peaks, as deduced by numerical second derivative of the data, are reported in Table II along with previous EELS (Ref. 30) and optical ellipsometric data.³¹

Since the absorption edge position of the ordered (1 ML Sb)/GaAs(110) shifts only by 30 meV with respect to the clean GaAs(110) surface, the semimetal-induced states do not extend significantly in the gap. On the contrary, in the Bi/GaAs(110) (Ref. 11) and the Sb/InP(110) (Refs. 8 and 27) interfaces, the semimetal-induced states can be both theoretically and experimentally found within the bulk gap, while in the present case the Sb-induced states are resonant with projected bulk band levels for most of the SBZ. Referring to the energy-level positions from direct photoemission data,⁹ we can very likely ascribe the 1.55-eV loss feature to an electronic transition between S6 and S7 Sb-induced states and the peak at 1.9 eV, also observed in previous EELS data,³⁰ is probably due to an S5-S7 transition (considering S7 degenerate with the CBM). Taking into account the available two-dimensional band-structure calculations,^{7,8} we do not

achieve an unequivocal attribution for the Sb-induced states involved in the electronic excitations, in the higher energy-loss region. However, the 2.3- and 2.6-eV structures might be due to an S5→S8 and to an S6→S8 excitation, respectively, at the \bar{X} point of the SBZ in agreement with pseudopotential calculations.⁷ The higher energy excitations at 3.2 and at 3.6 eV correspond fairly well to the previous experimental results^{30,31} reported in Table II.

The presence of additional electronic states due to defects and/or disorder during the formation of the monolayer are detectable for the Sb/GaAs only as a slight tail

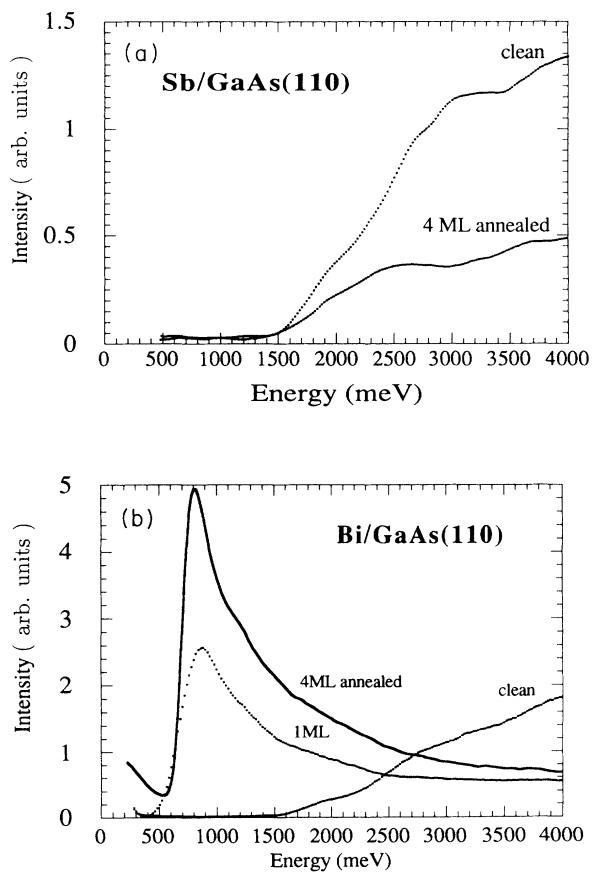


FIG. 2. (a) Comparison between the HREEL spectra of the clean GaAs(110) surface and the (1×1) Sb ordered monolayer. (b) Comparison among the HREEL spectra of the clean GaAs(110) surface, 1 ML Bi as deposited, and the Bi overlayer after the thermal treatment.

TABLE II. Energy-loss positions for (one ordered monolayer Sb)/GaAs(110), as measured in this work [HREELS, see Fig. 2(a)] compared with the transition energies as measured by electron-energy-loss-spectroscopy (Ref. 24) (EELS performed with a primary beam energy of about 100 eV) and ellipsometry (Ref. 31).

Sb/GaAs(110)						
HREELS	1.55	1.9	2.3	2.6	3.2	3.6
EELS (Ref. 24)		2.0	2.3			3.4
Ellipsometry (Ref. 31)				2.65	3.2	3.75

in the region of the bulk gap. After the annealing procedure the tail disappears, confirming the absence of a detectable joint density of additional states in the gap when the Sb monolayer is ordered.

For the Bi/GaAs(110) interface the annealing of the 4 ML of Bi was performed following an analogous procedure. The Bi in excess of 1 ML desorbs and leaves an epitaxial monolayer with a regular array of dislocations. The LEED pattern reflects the periodicity of the misfits, showing two slight extra spots in the $[1\bar{1}0]$ direction. These sixth-order spots correspond to a six-unit cell periodicity (24 Å) along the $[1\bar{1}0]$ direction. Since their intensity is weaker than that of the integer order diffraction spots, from previous LEED results^{12,19} it was deduced that the primary periodicity remains the (1×1) . The sharpness of the pattern and the presence of the extra spots suggest an ordered array of dislocations along the $[001]$ direction after the thermal treatment. The annealing procedure does not induce a more reflecting surface as deduced by the elastic peak intensity.

As shown in Fig. 2(b), after the annealing procedure, the absorption feature appears narrower and the main peak shifts by 50 meV to lower energy with respect to the one Bi monolayer as deposited.

Below the absorption edge, a broad feature is present. An analogous absorption feature, due to acceptorlike states, has been observed in the energy region of the bulk gap, for Bi deposited at room temperature on *p*-type GaAs(110).²⁸ STM spectroscopic results^{4,5} associated such states to the dangling and broken bonds near the dislocations. After the annealing treatment, since the ordered array of dislocations can induce an extended state over all the SBZ with a high density of states, such a structure becomes evident also on *n*-type substrates [Fig. 2(b)]. A detailed analysis of these properties is discussed elsewhere.²⁸

In the following we describe the HREEL results of the thick semimetallic overlayers on GaAs(110).

The Sb and Bi overlayers were evaporated in variable steps up to a few tens of ML. For each of these coverages the LEED pattern, the elastic peak intensity, and the vibrational properties of the substrate are evaluated to enlighten the evolution of the dielectric properties during the thick layer formation.

In the initial chemisorption stages a sharp (1×1) LEED pattern was observed and for coverages up to 1 ML a structureless background appeared, preserving the presence of intense (1×1) diffraction spots, for both Sb/GaAs(110) and Bi/GaAs(110), as already discussed.

Above 1 ML, the LEED pattern is different for the two interfaces, in fact for the Bi/GaAs(110) the (1×1) structure coexists with superstructures present at different coverages,^{12,13,19} while for the Sb/GaAs the (1×1) LEED spots are present until 10 ML, without superstructures, and disappear at 15 ML.^{14,15}

As shown in Fig. 3(a), the elastic peak intensity has a slight decrease when one Sb monolayer is deposited on GaAs(110), while a clear intensity reduction is observed in the same coverage range in correspondence of which the LEED pattern loses the sharpness and the background starts growing (4–10 ML). At 15 ML, when the LEED pattern disappears, the elastic peak intensity drops. This confirms the absence of long-range order for the Sb overlayer. In fact, after the formation of the epi-

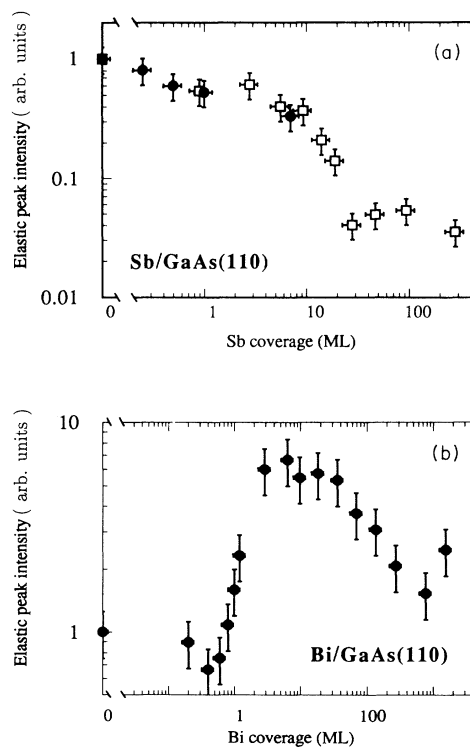


FIG. 3. (a) Elastic-scattering peak intensity as a function of the Sb coverage (dots: this experiment; squares: Ref. 14). (b) Elastic-scattering peak intensity as a function of the Bi coverage.

taxial monolayer the growth morphology is characterized by an amorphous phase with a Stranski-Krastanov growth up to the critical coverage of 15 ML, when the thick layer becomes polycrystalline.^{14,15}

Above 1 ML the Bi overlayer shows a different behavior. In particular, between 2 and 5 ML, a superstructure appears in the LEED image with slight extra spots along the diagonal $[1\bar{1}1]$ and $[\bar{1}11]$ directions. At this coverage range, the elastic peak intensity has a huge increase (one order of magnitude with respect to the clean surface), as shown in Fig. 3(b). This behavior cannot be explained with a more ordered structure with respect to the clean surface, but depends on the higher metallicity of the interface. In fact the surface reflectivity, related to the intensity of the reflected electron beam, depends not only on the surface order but also on the dielectric nature of the surface.

The elastic peak intensity presents an attenuation above 7 ML of Bi, and beyond 10 ML two slightly rotated hexagonal-like LEED images distinctly appear superimposed to the (1×1) pattern. Resch, Esser, and Richter¹⁹ explained this LEED pattern with trigonal symmetry caused by Bi facets having their C3 axis perpendicular to the surface and tilted by 10° with respect to the $[110]$ direction in the substrate $(1\bar{1}0)$ plane.

At higher coverages, the growth remains crystalline with a hexagonal-like LEED pattern and the elastic peak intensity slightly decreases above 30 ML.

The evidence of a more metallic character for the Bi/GaAs with respect to the Sb/GaAs system in the same coverage range (2–10 ML) is confirmed by the overlayer screening effect of the substrate vibrational structures. The Fuchs-Kliwer phonon is a surface optical phonon present in all surfaces of the III-V semiconductor compounds. On increasing the Sb deposition, the phonon frequency remains at about 36 meV as in the clean GaAs(110) surface, while its intensity decreases.¹⁴ Within the hypothesis that the overlayer is uniform and metallic the Fuchs-Kliwer phonon is expected to disappear before the completion of one monolayer. In fact, a metallic overlayer would strongly screen the dipole effective charge associated with the Fuchs-Kliwer mode. In previous works^{24,25} we analyzed with a three-layer dielectric model the effect of a semiconducting overlayer on the GaAs(110) phonon and the intensity behavior was fairly well reproduced for the Sb/GaAs(110) interface. During the crystallization process, above 15 Sb monolayers, metallic island nucleation in the Sb amorphous semiconducting layer takes place. The presence of the metallic islands is supported by the increase in the elastic peak width as discussed by Mariani, Annovi, and del Pennino.²⁵ When the metallic islands eventually coalesce the polycrystalline transition is completed.

For the Bi/GaAs(110) interface the phonon intensity decreases by one order of magnitude in the 1–10-ML coverage range,³² while for Sb the same attenuation is present only above 10 ML, as shown in Fig. 4. After the completion of one monolayer the more ordered growth morphology for the Bi/GaAs(110) interface—with respect to the Sb/GaAs(110)—gives rise to the formation of semimetallic islands which screen the dipole effective

charge of the Fuchs-Kliwer mode. Since the Fuchs-Kliwer phonon is still detectable at 10 ML, i.e., the attenuation rate is not that of a uniform metallic overlayer, the Bi metallic islands probably take up only a portion of the first semiconducting layer. In the same coverage range the metallic behavior is confirmed by the huge enhancement of the elastic peak.

The main differences in the growth morphology of Sb and Bi are summarized as follows.

(i) Bi overlayers between 2 and 7 ML present a more metallic character with respect to Sb clusters, while above 10 ML the dielectric properties of the Sb and Bi overlayers become similar.

(ii) The presence of the superstructures in the LEED images for Bi thick layer until high coverages indicates the presence of a long-range order in the Bi layer, absent for the Sb overlayer above 4 ML.

In the coverage region above 1 ML, where the growth morphology of the two semimetal/GaAs(110) systems show different behavior, it is also interesting to relate the structural properties and the dielectric nature of the overlayers to the electronic structure.

For Sb/GaAs(110) the HREEL spectra, for coverages above 1 ML, are shown in Fig. 5(a). At 2 ML, the presence of a tail in the band gap increases, leading to the presence of induced state in the gap. At 7 ML the approximate band-gap width is about 0.5 eV. Scanning tunneling spectroscopic results¹⁷ observed a very low conductivity in the energy region of the bulk gap when 10 ML of Sb are deposited on GaAs(110). The width of this “approximate band gap” is in agreement with our data although the authors cannot exclude a low conductivity near the Fermi level. They ascribed this behavior to the semimetallic properties of the Sb overlayer.

From our data, the existence of the gap in this coverage range confirms the semiconducting phase of the Sb/GaAs(110) interface. Moreover, as previously described, the presence of the substrate Fuchs-Kliwer phonon reveals the semiconducting character of the overlayer that cannot screen the dipole effective charge of the optical Fuchs-Kliwer mode.

For the Bi/GaAs interface at 2.1 ML of Bi we observe a continuum of transitions in the energy region of the

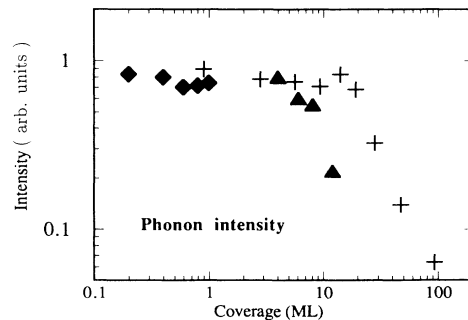


FIG. 4. Fuchs-Kliwer phonon intensity as a function of Sb (crosses: Ref. 14) and Bi (squares: this experiment; triangles: Ref. 32) coverages.

semiconductor gap as shown in Fig. 5(b). On increasing the Bi coverage, the gap disappears and the semimetallic character is confirmed. In a semimetallic system, the Fermi energy crosses the conduction band only in a few points of the Brillouin zone and the electronic structure can present energy gaps. Electronic transitions across the gaps can be observed superimposed to a continuum of intraband transitions. The energy position of the absorption feature shifts by 90 meV to lower energy on increasing the Bi coverage, even after the subtraction of the in-

traband contribution with a spline fit procedure. The semimetallic character (at 2.1 ML of Bi) confirms previous inverse photoemission results. In fact, Hu *et al.* show an emission at E_f [at 2.0 ML of Bi on GaAs (110)] and they did not report any significant change in relation with the Fermi-level position at higher coverages.

The evolution of the HREEL electronic structure, between 2 and 7 ML, absent in the bulk-Bi electronic structure, indicates that this crystalline and semimetallic phase is not comparable with the electronic properties of the bulk Bi. The semimetallic character of 2.1 ML of Bi confirms previous inverse photoemission results, in fact, Hu *et al.*¹³ show an emission at E_F at 2.0 ML and they did not report any significant change in relation with the Fermi-level position at higher coverages.

CONCLUSIONS

We presented a HREELS study of the Bi/GaAs(110) and Sb/GaAs(110) interface systems grown at room temperature, in a wide coverage range. Such interfaces were chosen inasmuch as they outline prototypic examples of epitaxial growth, at the monolayer scale. The structural similarity of both systems is reflected in their respective electronic properties. In particular, the first monolayers of Bi and Sb are semiconducting. However, although the scheme and the sequence of the semimetal-induced electronic levels are similar for both the interfaces, we found states in the gap in the (1 ML Bi)/GaAs(110) system, while we have no evidence of gap states in the (1 ML Sb)/GaAs(110). Additional states within the gap have been found by preparing 1 ML of Bi out of a thicker layer via appropriate thermal treatment. Such levels are correlated to dislocations inherent to the (1 ML Bi)/GaAs(110) system, which undergoes a long-range ordering, as deduced by LEED.

The two interfaces present different growth morphology at the higher coverages, leading to different electronic and dielectric properties. The latter were deduced by evaluating the screening exerted by the overlayer onto the substrate's Fuchs-Kliever phonon. Antimony grows as an amorphous and nonmetallic layer up to about 15 ML, presenting a semiconducting gap, in agreement with STM spectroscopic results. On the other hand, bismuth grows in an ordered metastable crystalline phase between 2 and 10 ML, with a definite semimetallic character manifested by the presence of interband transitions superimposed to a continuum of intraband transitions. At higher thickness both the systems evolve to a semimetallic bulk-like stage, though Sb remains polycrystalline while Bi grows in a single-crystal morphology.

ACKNOWLEDGMENTS

Experimental assistance from E. Angeli is gratefully acknowledged. Financial grants came partially from Consiglio Nazionale delle Ricerche (CNR), and Ministero dell'Università e della Ricerca Scientifica e Tecnologica (MURST).

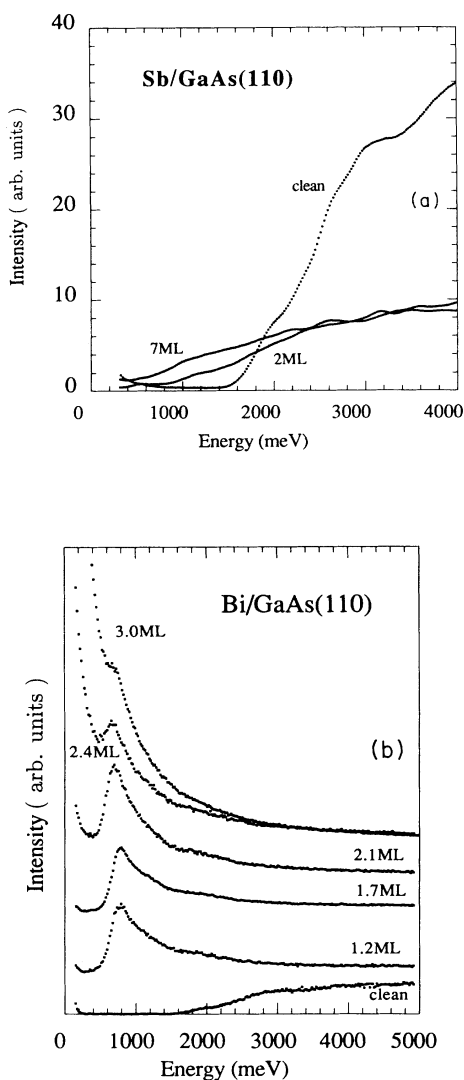


FIG. 5. (a) High-resolution electron-energy-loss spectra of the Sb/GaAs(110) system, as a function of Sb coverage (2–7 ML) in the energy region of the fundamental bulk gap. Primary beam energy $E_p = 15.9$ eV; angle of incidence $\theta_i = 65^\circ$. Spectra are normalized to the respective elastic-scattering peak heights. (b) High-resolution electron-energy-loss spectra of the Bi/GaAs(110) system, as a function of Bi coverage (1.2–3.0 ML) in the energy region of the fundamental bulk gap. Primary beam energy $E_p = 12$ eV; angle of incidence $\theta_i = 65^\circ$. Spectra are normalized to the respective elastic-scattering peak heights.

- ¹J. Carelli and A. Kahn, *Surf. Sci.* **116**, 280 (1982).
- ²W. K. Ford, T. Guo, D. L. Lessor, and C. B. Duke, *Phys. Rev. B* **42**, 8925 (1990), and references therein.
- ³T. Guo, R. E. Atkinson, and W. K. Ford, *Phys. Rev. B* **41**, 5138 (1990).
- ⁴R. M. Feenstra and P. Mårtensson, *Phys. Rev. Lett.* **61**, 447 (1988).
- ⁵R. Ludeke, A. Taleb-Ibrahimi, R. M. Feenstra, and A. B. McLean, *J. Vac. Sci. Technol. B* **7**, 936 (1989).
- ⁶A. B. McLean, R. M. Feenstra, A. Taleb-Ibrahimi and R. Ludeke, *Phys. Rev. B* **39**, 12 925 (1989).
- ⁷C. M. Bertoni, C. Calandra, F. Manghi, and E. Molinari, *Phys. Rev. B* **27**, 1251 (1983).
- ⁸C. Mailhot, C. B. Duke, and D. J. Chadi, *Phys. Rev. B* **31**, 2213 (1985).
- ⁹A. Tulke, Monika Mattern Klosson, and H. Lüth, *Solid State Commun.* **59**, 303 (1986).
- ¹⁰W. Drube and F. J. Himpsel, *Phys. Rev. B* **37**, 855 (1988).
- ¹¹A. B. McLean, R. Ludeke, M. Prietsch, D. Heskett, D. Tang, and T. Maeda Wong, *Phys. Rev. B* **43**, 7243 (1991).
- ¹²A. B. McLean and F. Himpsel, *Phys. Rev. B* **40**, 8425 (1989).
- ¹³Yongjun Hu, T. J. Wagener, M. B. Jost, and J. H. Weaver, *Phys. Rev. B* **40**, 1146 (1989); **41**, 5817 (1990).
- ¹⁴G. Annovi, Maria Grazia Betti, U. del Pennino, and C. Mariani, *Phys. Rev. B* **41**, 11 978 (1990).
- ¹⁵M. Hünermann, W. Pletschen, U. Resch, U. Rettweiler, W. Richter, J. Geurts, and P. Lautenschlager, *Surf. Sci.* **189/190**, 322 (1987); N. Esser, H. Münder, M. Hünermann, W. Pletschen, W. Richter, and D. R. T. Zahn, *J. Vac. Sci. Technol. B* **5**, 1044 (1987).
- ¹⁶D. E. Savage and M. G. Lagally, *Appl. Phys. Lett.* **50**, 1719 (1987).
- ¹⁷C. K. Shih, R. M. Feenstra, and P. Mårtensson, *J. Vac. Sci. Technol. A* **8**, 3379 (1990).
- ¹⁸J. J. Joyce, J. Anderson, M. M. Nelson, and G. J. Lapeyre, *Phys. Rev. B* **40**, 10 412 (1989).
- ¹⁹U. Resch, N. Esser, and W. Richter, *Surf. Sci.* (to be published).
- ²⁰N. Esser, M. Huenermann, U. Resch, D. Spaltmann, J. Geurts, D. R. T. Zahn, W. Richter, and R. H. Williams, *Appl. Surf. Sci.* **41/42**, 169 (1989).
- ²¹H. Ibach and D. L. Mills, *Electron Energy Loss Spectroscopy and Surface Vibrations* (Academic, New York, 1982).
- ²²U. del Pennino, M. G. Betti, C. Mariani, C. M. Bertoni, S. Nannarone, I. Abati, and A. Rizzi, *Surf. Sci.* **189/190**, 689 (1987).
- ²³U. del Pennino, Maria Grazia Betti, Carlo Mariani, and I. Abati, *ibid.* **207**, 133 (1988); S. Nannarone, S. D'Addato, J. A. Schaefer, Yu Chen, J. Anderson, and G. J. Lapeyre, *ibid.* **211/212**, 524 (1989).
- ²⁴Carlo Mariani, G. Annovi, U. del Pennino, Maria Grazia Betti, and M. Pedio, *J. Electron Spectrosc. Relat. Phenom.* **54/55**, 1105 (1990).
- ²⁵Carlo Mariani, G. Annovi, and U. del Pennino, *Surf. Sci.* **251/252**, 218 (1991).
- ²⁶M. G. Betti, M. Pedio, U. del Pennino, and C. Mariani, *Surf. Sci.* **251/252**, 209 (1991).
- ²⁷M. G. Betti, M. Pedio, U. del Pennino, and C. Mariani, *Phys. Rev. B* **43**, 14 317 (1991).
- ²⁸R. Compañó, U. del Pennino, C. Mariani, M. G. Betti, and M. Pedio, *Appl. Surf. Sci.* **56-58**, 242 (1992); R. Compañó, U. del Pennino, and C. Mariani, *Phys. Rev. Lett.* **68**, 986 (1992).
- ²⁹The energy position of the absorption edge in EELS is referred to the longitudinal frequency. It is at a higher energy with respect to the optical gap value (transverse frequency).
- ³⁰M. G. Betti, A. Campo, M. Capozzi, M. Pedio, P. Perfetti, and C. Quaresima, *Vuoto XX*, 75 (1990); R. Strümpfer and H. Lüth, *Surf. Sci.* **182**, 545 (1988).
- ³¹Monika Mattern-Klosson, R. Strümpfer, and H. Lüth, *Phys. Rev.* **33**, 2559 (1986).
- ³²C. Mariani, V. De Renzi, and R. Compañó, *Appl. Surf. Sci.* **56-58**, 247 (1992).